Valence properties of Cu and Ru in titanium-substituted $Ln\mathbf{Cu_3Ru_4O_{12}}$ (Ln = La, Pr, Nd) investigated by XANES and TGA

Stefan Riegg, Armin Reller, Alois Loidl, and Stefan G. Ebbinghaus

Supplemental information: Crystal-structure and XANES data of $Ln_y\mathbf{Cu_3Ru}_x\mathbf{Ti}_{4-x}\mathbf{O}_{12+\delta}$

1. Crystal-structure data

In Tab. 1 the cell parameters of the $Ln_y\mathrm{Cu_3Ru}_x\mathrm{Ti}_{4-x}\mathrm{O}_{12+\delta}$ samples are listed together with the relative atomic coordinates of oxygen x(O) and y(O). Furthermore, the values of the fit residuals ($\mathrm{R_p}$, $\mathrm{R_{wp}}$ in %) as well as χ^2 are given to compare the fit-quality of the Rietveld-refinement results. For the isotropic displacement factors fixed values were used ($A = Ln$: 0.7; A' = Cu: 0.5; B = Ru,Ti: 0.5; O = 1.0), only the overall isotropic $\mathrm{B_{ov}}$ was refined and has to be subtracted from the individual site B-values. In first attempts, the site occupation factors (SOF) of O, Cu, and Ru/Ti were fixed and the occupation of the Ln-site was allowed to vary, resulting in values very close to the nominal ones. For this reason, in the final calculations the SOF were not refined, instead they were set to the values calculated from the ratio of corresponding multiplicities according to the Wyckoff-notation.

The room temperature x-ray powder diffraction (XRD) patterns were recorded using a Seifert 3003 TT $\theta - \theta$ powder diffractometer (Cu-$\mathrm{K}_{\alpha 1,2}$ radiation) for the angular range $10° \leq 2\theta \leq 150°$. A one-dimensional single-line semiconductor detector (METEOR 1D) was used and a step width of 0.01° and an integration time of 300 s per data point was chosen. The samples marked with an asterisk (*) in Tab. 1 were recorded on the same diffractometer using a scintillation detector. For these measurements the angular range $10° \leq 2\theta \leq 100°$, a step width of 0.015°, and an integration time of 7 s per data point were used.

In Figs. 1 and 2 the XRD patterns of the $\mathrm{Pr}_y\mathrm{Cu_3Ru}_x\mathrm{Ti}_{4-x}\mathrm{O}_{12+\delta}$ and $\mathrm{Nd}_y\mathrm{Cu_3Ru}_x\mathrm{Ti}_{4-x}\mathrm{O}_{12+\delta}$ series are shown. In the upper frames a) representative results of the Rietveld refinement are depicted. To increase clarity in the lower frames b), the data were normalized to the intensity of (220) and shifted by a constant value. Very small peaks of trace-impurity phases were identified as $\mathrm{TiO_2/RuO_2}$ (at approximately 28° 2θ) and $Ln_2\mathrm{O_3}$ (at approximately 30° 2θ). The total amount of impurities is well below 1% of the sample weight as determined from XRD Rietveld analysis.

Table 2 lists relevant interatomic distances (in Å) and bond angles (in °). The error ranges amount to 0.03 Å for the distances and 1.2 degrees for the angles, respectively. The corresponding data of this table are depicted in Fig. 3 a - f.

Table 1. Results of the XRD-Rietveld refinement of $Ln_yCu_3Ru_xTi_{4-x}O_{12+\delta}$ (Space group $Im\bar{3}$). (* = measured with scintillation detector)

Sample	a (Å)	x(O)	y(O)	B_{ov}	R_p (%)	R_{wp} (%)	χ^2
$La_{0.67}Cu_3Ti_4O_{12}$*	7.4199(1)	0.1783(7)	0.3016(6)	-0.36(2)	6.11	7.60	1.46
$La_{0.77}Cu_3Ru_{0.1}Ti_{3.9}O_{12}$	7.4210(1)	0.1826(3)	0.3062(3)	-0.33(1)	3.01	4.51	4.15
$La_{0.92}Cu_3Ru_{0.25}Ti_{3.75}O_{12}$	7.4428(1)	0.1792(3)	0.3038(2)	-0.35(1)	2.61	3.68	3.04
$LaCu_3Ru_{0.33}Ti_{3.67}O_{12}$	7.4450(1)	0.1809(2)	0.3040(2)	-0.04(1)	2.67	3.88	3.53
$LaCu_3Ru_{0.5}Ti_{3.5}O_{12}$	7.4487(1)	0.1806(3)	0.3055(3)	-0.06(1)	2.06	3.03	5.68
$LaCu_3Ru_{1.0}Ti_{3.0}O_{12}$	7.4576(1)	0.1803(3)	0.3068(2)	-0.17(1)	1.63	2.26	3.85
$LaCu_3Ru_{1.5}Ti_{2.5}O_{12}$	7.4618(1)	0.1793(3)	0.3074(2)	-0.31(1)	1.38	1.85	2.93
$LaCu_3Ru_{2.0}Ti_{2.0}O_{12}$	7.4666(1)	0.1815(4)	0.3036(3)	-0.06(1)	1.19	1.62	2.78
$LaCu_3Ru_{2.25}Ti_{1.75}O_{12}$	7.4672(1)	0.1817(4)	0.3035(3)	-0.30(1)	1.16	1.55	2.70
$LaCu_3Ru_{2.5}Ti_{1.5}O_{12}$	7.4693(1)	0.1758(3)	0.3027(3)	-0.39(1)	1.37	1.95	3.99
$LaCu_3Ru_{3.0}Ti_{1.0}O_{12}$*	7.4707(2)	0.1771(9)	0.3047(7)	-0.81(4)	5.10	7.16	1.20
$LaCu_3Ru_{3.25}Ti_{0.75}O_{12}$	7.4733(1)	0.1759(4)	0.3035(3)	-0.50(1)	1.09	1.46	2.66
$LaCu_3Ru_{3.5}Ti_{0.5}O_{12}$*	7.4739(2)	0.1761(10)	0.3061(8)	-0.97(4)	5.77	7.41	1.19
$LaCu_3Ru_4O_{12}$*	7.4778(2)	0.1725(10)	0.2898(7)	-0.98(4)	6.65	8.56	1.48
$Pr_{0.67}Cu_3Ti_4O_{12}$*	7.4032(2)	0.1774(8)	0.3007(7)	-0.47(4)	5.93	7.45	1.40
$Pr_{0.77}Cu_3Ru_{0.1}Ti_{3.9}O_{12}$*	7.4037(2)	0.1843(7)	0.3040(6)	-0.07(4)	4.84	6.09	1.11
$Pr_{0.92}Cu_3Ru_{0.25}Ti_{3.75}O_{12}$*	7.4281(2)	0.1779(6)	0.3005(5)	-0.04(4)	6.77	8.52	1.61
$PrCu_3Ru_{0.33}Ti_{3.67}O_{12}$	7.4322(1)	0.1788(3)	0.3029(2)	-0.03(1)	2.67	3.87	6.93
$PrCu_3Ru_{0.5}Ti_{3.5}O_{12}$*	7.4329(3)	0.1802(7)	0.3069(6)	-0.28(4)	6.29	8.10	1.68
$PrCu_3Ru_{1.0}Ti_{3.0}O_{12}$*	7.4345(3)	0.1791(7)	0.3094(6)	-0.21(5)	6.22	7.91	1.60
$PrCu_3Ru_{2.0}Ti_{2.0}O_{12}$	7.4476(1)	0.1772(4)	0.3050(3)	-0.27(1)	1.79	2.71	5.48
$PrCu_3Ru_{3.0}Ti_{1.0}O_{12}$	7.4556(1)	0.1755(3)	0.3046(3)	-0.49(1)	1.41	1.87	3.02
$PrCu_3Ru_{3.5}Ti_{0.5}O_{12}$	7.4588(1)	0.1723(3)	0.3020(3)	-0.51(1)	1.44	2.00	2.19
$PrCu_3Ru_4O_{12}$	7.4628(1)	0.1719(5)	0.3048(4)	-0.84(1)	1.61	2.28	4.91
$Nd_{0.67}Cu_3Ti_4O_{12}$*	7.3988(2)	0.1782(9)	0.3017(8)	-0.45(4)	5.89	7.40	1.24
$Nd_{0.77}Cu_3Ru_{0.1}Ti_{3.9}O_{12}$*	7.4011(2)	0.1841(7)	0.3063(7)	-0.18(4)	5.12	6.44	1.14
$Nd_{0.92}Cu_3Ru_{0.25}Ti_{3.75}O_{12}$*	7.4121(2)	0.1816(6)	0.3027(5)	0.04(4)	4.85	6.10	1.08
$NdCu_3Ru_{0.33}Ti_{3.67}O_{12}$*	7.4256(2)	0.1796(7)	0.3030(6)	-0.09(5)	5.39	6.74	1.26
$NdCu_3Ru_{0.5}Ti_{3.5}O_{12}$*	7.4299(2)	0.1800(6)	0.3048(5)	-0.20(4)	5.84	7.33	1.37
$NdCu_3Ru_{0.75}Ti_{3.25}O_{12}$*	7.4277(3)	0.1789(6)	0.3045(5)	-0.15(4)	5.05	6.37	1.10
$NdCu_3Ru_{1.0}Ti_{3.0}O_{12}$	7.4390(1)	0.1780(3)	0.3047(2)	-0.24(1)	2.29	3.49	4.46
$NdCu_3Ru_{1.25}Ti_{2.75}O_{12}$*	7.4408(3)	0.1780(7)	0.3052(6)	-0.07(4)	5.30	6.77	1.23
$NdCu_3Ru_{2.0}Ti_{2.0}O_{12}$*	7.4401(3)	0.1779(8)	0.3051(7)	-0.38(4)	6.48	8.13	1.49
$NdCu_3Ru_{3.0}Ti_{1.0}O_{12}$	7.4497(1)	0.1745(3)	0.3042(2)	-0.38(1)	1.46	1.97	3.35
$NdCu_3Ru_{3.15}Ti_{0.85}O_{12}$	7.4512(1)	0.1735(3)	0.3040(3)	-0.34(1)	1.42	1.96	2.06
$NdCu_3Ru_{3.25}Ti_{0.75}O_{12}$	7.4520(1)	0.1733(3)	0.3044(2)	-0.34(1)	1.37	1.91	1.98
$NdCu_3Ru_{3.35}Ti_{0.65}O_{12}$	7.4525(1)	0.1743(3)	0.3038(2)	-0.35(1)	1.42	2.04	2.31
$NdCu_3Ru_{3.5}Ti_{0.5}O_{12}$	7.4529(1)	0.1768(3)	0.3020(2)	-0.49(4)	1.42	1.89	3.27
$NdCu_3Ru_4O_{12}$	7.4574(1)	0.1749(4)	0.3026(3)	-0.50(1)	1.44	1.97	3.67

Table 2. Interatomic distances and bond angles derived from XRD-Rietveld refinement of $Ln_yCu_3Ru_xTi_{4-x}O_{12+\delta}$ (Space group $Im\bar{3}$). The error ranges amount to 0.03 Å for the distances and 1.2 degrees for the angles, respectively.

Sample	*Ln*–O (Å)	Ru–O (Å)	Cu–O (Å)	Ru–O–Ru (°)	Cu–O–Ru (°)	O–Cu–O (°)
$La_{0.67}Cu_3Ti_4O_{12}$	2.604	1.965	1.982	141.3	108.9	95.7
$La_{0.77}Cu_3Ru_{0.1}Ti_{3.9}O_{12}$	2.685	1.964	1.979	141.7	109.1	90.9
$La_{0.92}Cu_3Ru_{0.25}Ti_{3.75}O_{12}$	2.685	1.973	1.975	141.1	109.4	91.6
$LaCu_3Ru_{0.33}Ti_{3.67}O_{12}$	2.687	1.973	1.978	141.2	109.4	91.5
$LaCu_3Ru_{0.5}Ti_{3.5}O_{12}$	2.681	1.977	1.970	140.7	109.6	92.1
$LaCu_3Ru_{1.0}Ti_{3.0}O_{12}$	2.672	1.982	1.967	140.4	109.7	92.9
$LaCu_3Ru_{1.5}Ti_{2.5}O_{12}$	2.673	1.985	1.963	140.1	109.9	93.0
$LaCu_3Ru_{2.0}Ti_{2.0}O_{12}$	2.637	1.976	1.999	141.7	108.9	94.8
$LaCu_3Ru_{2.25}Ti_{1.75}O_{12}$	2.652	1.975	1.999	141.8	108.9	93.8
$LaCu_3Ru_{2.5}Ti_{1.5}O_{12}$	2.635	1.996	1.945	138.6	110.3	95.9
$LaCu_3Ru_{3.0}Ti_{1.0}O_{12}$	2.618	1.989	1.969	139.7	109.6	96.6
$LaCu_3Ru_{3.25}Ti_{0.75}O_{12}$	2.632	1.988	1.974	140.1	109.6	95.6
$LaCu_3Ru_{3.5}Ti_{0.5}O_{12}$	2.646	2.000	1.938	138.2	110.5	95.5
$LaCu_3Ru_4O_{12}$	2.630	1.992	1.966	139.6	109.8	96.0
$Pr_{0.67}Cu_3Ti_4O_{12}$	2.586	1.963	1.975	141.0	109.0	96.6
$Pr_{0.77}Cu_3Ru_{0.1}Ti_{3.9}O_{12}$	2.723	1.963	1.965	141.1	109.4	91.5
$Pr_{0.92}Cu_3Ru_{0.25}Ti_{3.75}O_{12}$	2.547	1.974	1.984	140.3	108.7	99.5
$PrCu_3Ru_{0.33}Ti_{3.67}O_{12}$	2.646	1.972	1.973	140.9	109.4	93.7
$PrCu_3Ru_{0.5}Ti_{3.5}O_{12}$	2.654	1.977	1.958	140.1	109.8	93.5
$PrCu_3Ru_{1.0}Ti_{3.0}O_{12}$	2.663	1.984	1.940	139.1	110.3	93.4
$PrCu_3Ru_{2.0}Ti_{2.0}O_{12}$	2.644	1.982	1.961	140.0	109.8	94.5
$PrCu_3Ru_{3.0}Ti_{1.0}O_{12}$	2.645	1.984	1.964	140.0	109.7	94.6
$PrCu_3Ru_{3.5}Ti_{0.5}O_{12}$	2.609	1.987	1.964	139.6	109.7	96.9
$PrCu_3Ru_4O_{12}$	2.645	1.993	1.945	139.8	110.3	95.1
$Nd_{0.67}Cu_3Ti_4O_{12}$	2.595	1.962	1.973	141.1	109.0	96.0
$Nd_{0.77}Cu_3Ru_{0.1}Ti_{3.9}O_{12}$	2.644	1.958	1.978	141.8	109.0	92.9
$Nd_{0.92}Cu_3Ru_{0.25}Ti_{3.75}O_{12}$	2.659	1.961	1.979	141.7	109.1	92.3
$NdCu_3Ru_{0.33}Ti_{3.67}O_{12}$	2.671	1.967	1.974	141.3	109.3	92.0
$NdCu_3Ru_{0.5}Ti_{3.5}O_{12}$	2.636	1.972	1.969	140.7	109.4	94.3
$NdCu_3Ru_{1.0}Ti_{3.0}O_{12}$	2.630	1.975	1.963	140.3	109.6	94.8
$NdCu_3Ru_{2.0}Ti_{2.0}O_{12}$	2.616	1.975	1.978	140.7	109.2	95.8
$NdCu_3Ru_{3.0}Ti_{1.0}O_{12}$	2.627	1.984	1.959	139.7	109.8	95.6
$NdCu_3Ru_{3.5}Ti_{0.5}O_{12}$	2.620	1.978	1.980	140.7	109.2	95.7
$NdCu_3Ru_4O_{12}$	2.612	1.985	1.967	139.8	109.6	96.6

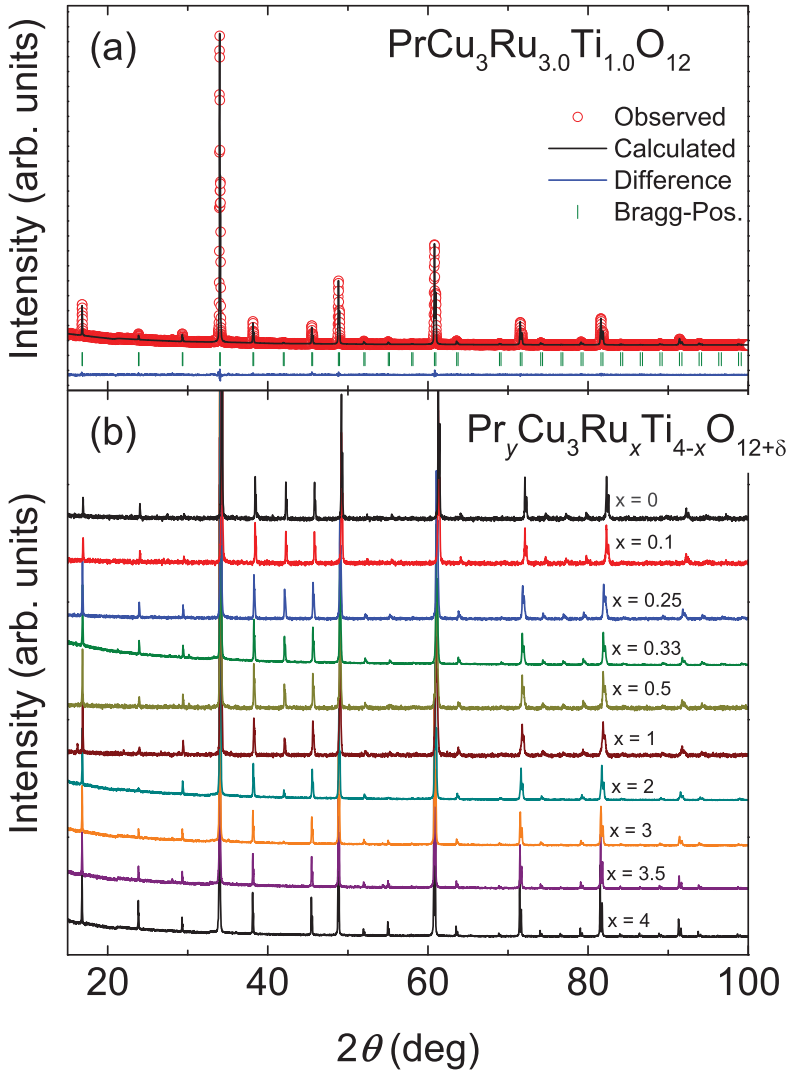

Figure 1. (a) Representative Rietveld-refinement of the x-ray diffraction pattern of $PrCu_3Ru_{3.0}Ti_{1.0}O_{12}$ measured at room temperature. (b) X-ray diffraction patterns of $Pr_yCu_3Ru_xTi_{4-x}O_{12+\delta}$ for different Ru contents x, normalized to the intensity of (2 2 0).

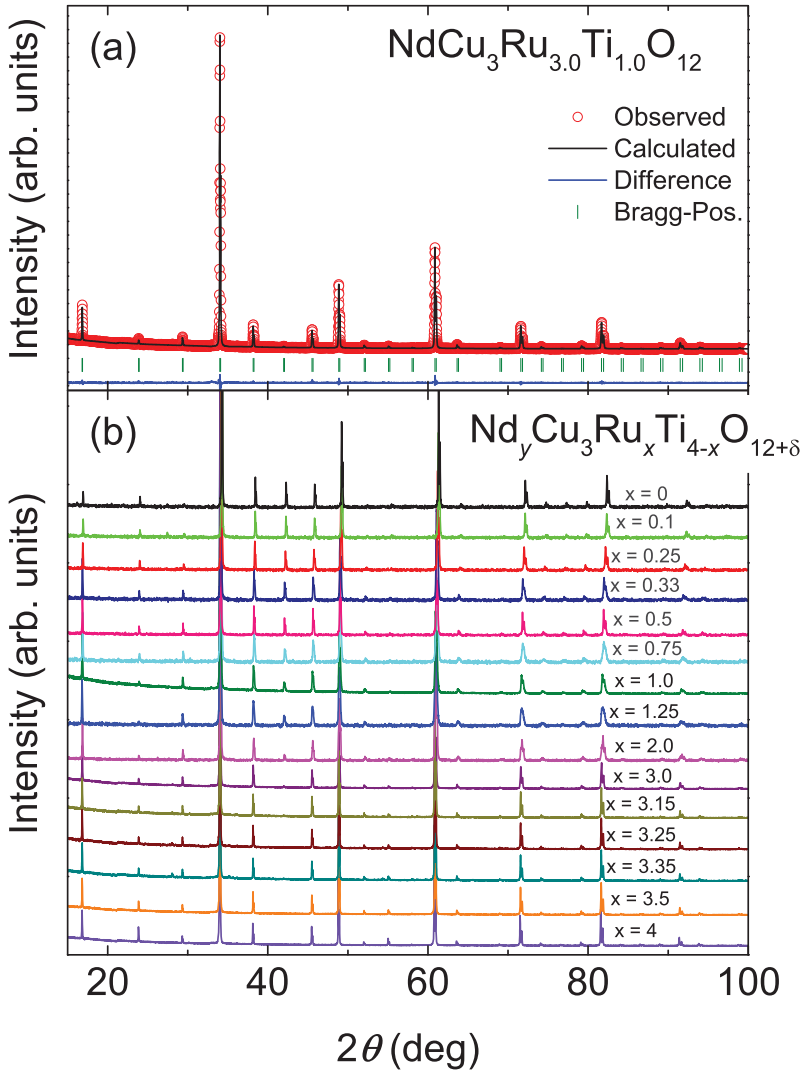

Figure 2. (a) Representative Rietveld-refinement of the x-ray diffraction pattern of $NdCu_3Ru_{3.0}Ti_{1.0}O_{12}$ measured at room temperature. (b) X-ray diffraction patterns of $Nd_yCu_3Ru_xTi_{4-x}O_{12+\delta}$ for different Ru contents x, normalized to the intensity of (2 2 0).

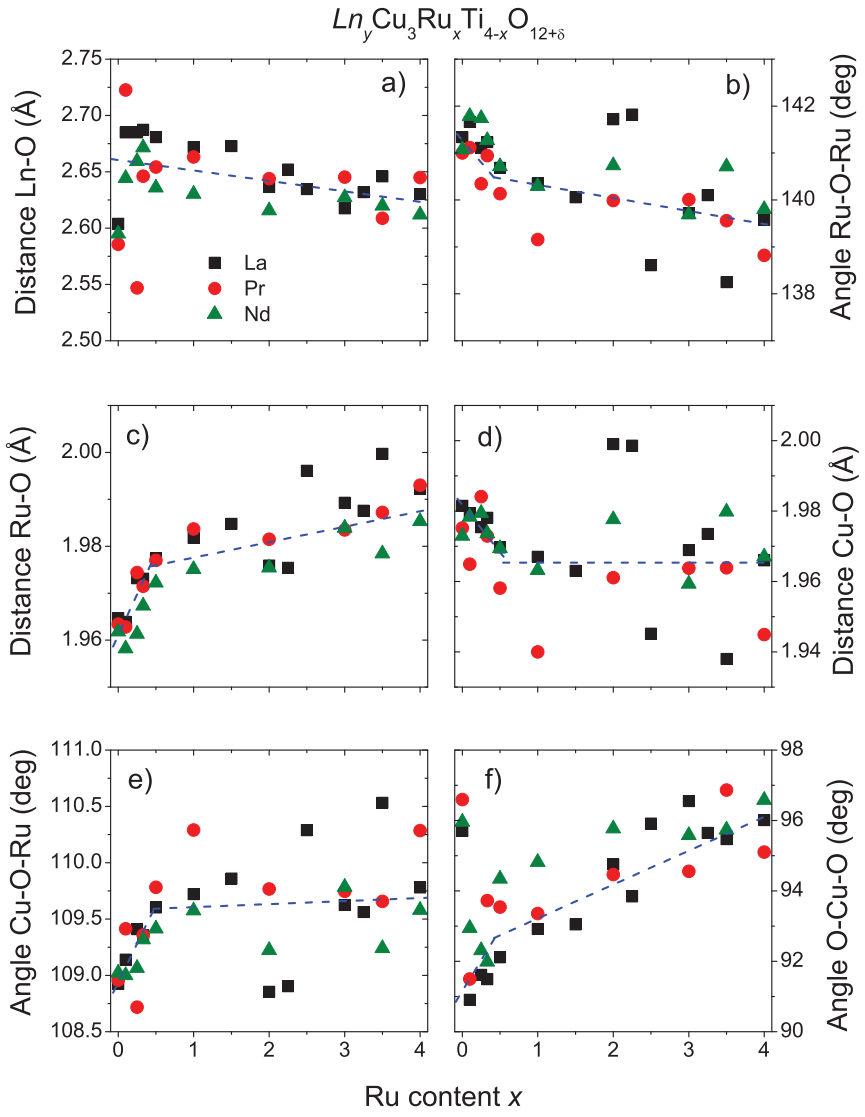

Figure 3. Structural data of $Ln_yCu_3Ru_xTi_{4-x}O_{12+\delta}$. a) Ln–O distances, b) Ru–O–Ru angles, c) Ru–O bond lengths, d) Cu–O bond lengths, e) Cu–O–Ru angles, and f) O–Cu–O angles. Dashed blue lines are drawn to guide the eye.

2. XANES data

Fig. 4 shows the Ru-K edge XANES spectra for $Ln_yCu_3Ru_xTi_{4-x}O_{12+\delta}$ after background subtraction and normalization. The spectra are grouped for the rare-earth metal La, Pr, and Nd and the groups are shifted by a constant value to increase clarity. The spectra are shown for ruthenium concentrations $x = 0.5$ (only La), 1.0, 2.0, 3.0, 4.0. The A-site substitution does not remarkably influence the shape of the XANES spectra and significant deviations caused by the increasing Ru concentration are not observed, either.

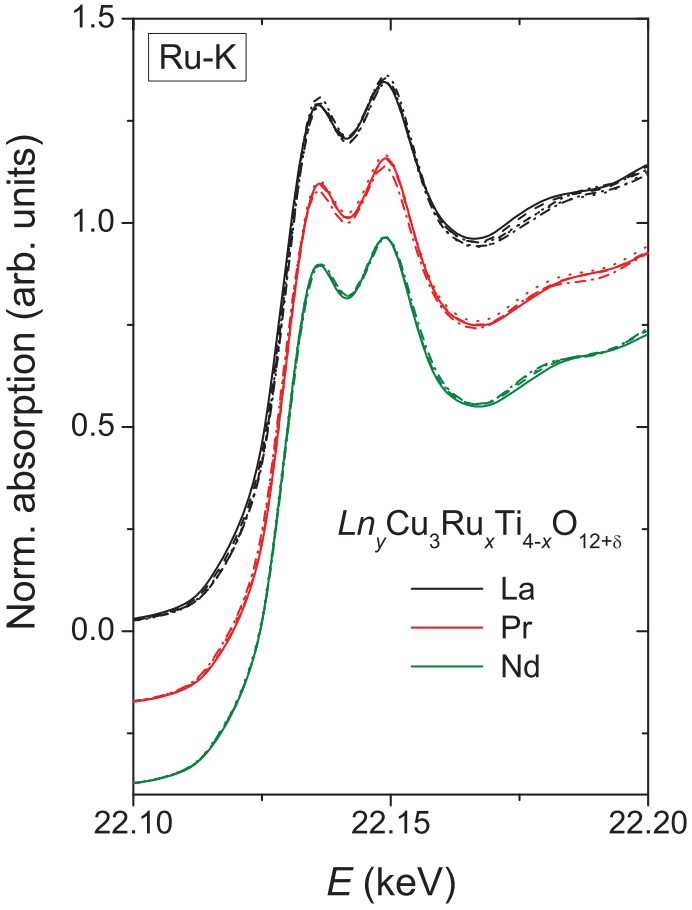

Figure 4. Ru-K edge XANES spectra of $Ln_yCu_3Ru_xTi_{4-x}O_{12+\delta}$ for the three investigated A-site rare-earth elements: La (top), Pr (center), Nd (bottom). The spectra are grouped for each element and each group is shifted by a constant value to increase clarity.